Theoretical and Applied Mechanics Letters 5 (2015) 9–12

Contents lists available at ScienceDirect

Theoretical and Applied Mechanics Letters

journal homepage: www.elsevier.com/locate/taml

Letter

Propulsive performance of two- and three-dimensional flapping flexible plates

Chao Tang, Xiyun Lu *

Department of Modern Mechanics, University of Science and Technology of China, Hefei 230026, China

ARTICLE INFO

Article history:
Received 21 November 2014
Received in revised form
30 December 2014
Accepted 1 January 2015
Available online 14 February 2015
*This article belongs to the Fluid Mechanics

Keywords:
Flapping-based locomotion
Self-propulsion
Flexible plate
Passive deformation
Fluid–structure interaction

ABSTRACT

The propulsive performance of two- and three-dimensional (2D and 3D) flapping flexible plates in a fluid at rest is investigated by a finite element method for the plate motion and an immersed boundary-lattice Boltzmann method for the fluid flow. We consider a model that as the leading-edge of the plate takes a vertical oscillation, the entire plate moves freely due to the fluid–structure interaction. The effects of flexibility on the dynamics of the 2D and 3D flapping plates are investigated. It is found that a suitable flexibility is benefit for improving the propulsive performance. The results obtained in this study provide physical insight into the understanding of the dynamics of the flapping-based locomotion.

© 2015 The Authors. Published by Elsevier Ltd on behalf of The Chinese Society of Theoretical and Applied Mechanics. This is an open access article under the CC BY-NC-ND license (http://creativecommons.org/licenses/by-nc-nd/4.0/).

A common strategy of swimming or flying animals for locomotion is to use their fins or wings to make flapping motions [1–3]. The wings and fins have complex behaviors which are associated with the distribution of the compliant components [1,4] and can deform passively in response to fluid forces [5–8]. The deformations in turn affect the propulsive performances [9]. In reality the role of flexibility in the flapping-based locomotion is still completely unclear and is of great interest for future detailed studies. Moreover, the mechanical properties of wings and fins have been measured which can be used to provide a physical basis for establishing a reliable model.

For animals in free flight or swimming, the mean thrust generated balances the resistance experienced by the surrounding fluid. The dynamical behaviors related to the free motion should be studied. Actually, the physical models considered in extensive work are an object immersed in a given uniform incoming flow, and the relevant fluid dynamics is different from a free moving object in a stationary fluid [10]. Some efforts have been done to study the locomotion of flapping flexible bodies in a stationary fluid. The two-dimensional (2D) simulation and modeling of the lamprey swimming were performed [11]. The dynamics of a 2D heaving plate with passive pitching motion was investigated [12,13]. However, since the instantaneous shape of an elastic structure in free motion depends on the local passive deformation due to the fluid–structure interaction [9], a model of a three-dimensional (3D) flexible wing moving passively in a stationary fluid is needed to be considered.

The 3D effect has an important influence on the dynamic performance and vortical structures of flapping plates [14]. Recently, the 3D effects on the translational locomotion of a passive heaving wing have been investigated [15]. However, the most previous studies of the locomotion of flapping flexible plate mainly focus on the 2D model [9,16,17]. Therefore, the propulsive performances of the 2D and 3D flexible plates are desirable to be studied.

In this study, we consider a flexible plate with length c and span length R in a stationary fluid. As shown in Fig. 1, the leading-edge is forced to perform a vertical oscillation

$$h(t) = A_0 \cos(2\pi f t), \tag{1}$$

where A_0 is the oscillating amplitude and f the frequency. As a result of the interplay of the plate elasticity, the leading-edge forcing, and the forces exerted by the surrounding fluid, the plate starts to move freely and passively in the stationary fluid. The active pitching angle is zero in this model. The passive pitching angle α can be defined as the angle between the x-axis and the secant connecting the leading-edge to the trailing-edge in the mid-span plane.

To investigate this system of the fluid and flexible plate interaction, the incompressible Navier–Stokes equations are used

* Corresponding author.
E-mail address: xlu@ustc.edu.cn (X. Lu).

http://dx.doi.org/10.1016/j.taml.2015.02.001
2095-0349/© 2015 The Authors. Published by Elsevier Ltd on behalf of The Chinese Society of Theoretical and Applied Mechanics. This is an open access article under the CC BY-NC-ND license (http://creativecommons.org/licenses/by-nc-nd/4.0/).

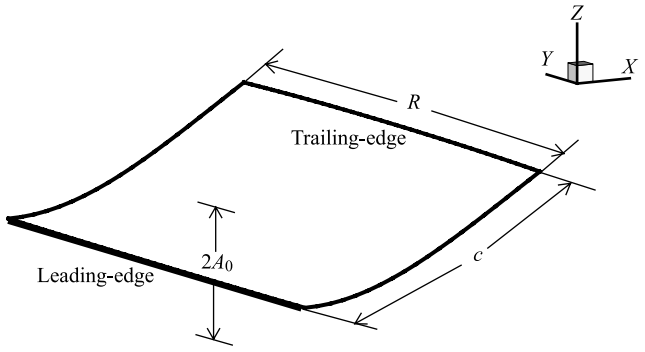

Fig. 1. Schematic of the 3D flapping flexible plate.

to simulate the fluid flow,

$$\frac{\partial \boldsymbol{v}}{\partial t} + \boldsymbol{v}\cdot\nabla\boldsymbol{v} = -\frac{1}{\rho}\nabla p + \frac{\mu}{\rho}\nabla^2\boldsymbol{v} + \boldsymbol{f}, \tag{2}$$

$$\nabla\cdot\boldsymbol{v} = 0, \tag{3}$$

where $\boldsymbol{v}$ is the velocity, p the pressure, ρ the density of the fluid, μ the dynamic viscosity, and $\boldsymbol{f}$ the body force term. The structural equation is used to describe the plate deformation and motion [18]

$$\rho_s h\frac{\partial^2 \boldsymbol{X}}{\partial t^2} = \sum_{i,j=1}^{2}\left\{\frac{\partial}{\partial s_i}\left\{Eh\varphi_{ij}\left[\delta_{ij} - \left(\frac{\partial \boldsymbol{X}}{\partial s_i}\cdot\frac{\partial \boldsymbol{X}}{\partial s_j}\right)^{-1/2}\right]\frac{\partial \boldsymbol{X}}{\partial s_j}\right.\right.$$
$$\left.\left. - \frac{\partial}{\partial s_j}\left(EI\gamma_{ij}\frac{\partial^2 \boldsymbol{X}}{\partial s_i \partial s_j}\right)\right\}\right\} + \boldsymbol{F}_s, \tag{4}$$

where $\boldsymbol{X}$ is the position vector of the plate, $\boldsymbol{F}_s$ is the Lagrangian force exerted on the plate by the fluid, Eh and EI are the stretching and bending stiffness of the plate, φ_{ij} and γ_{ij} are the in-plane and out-of-plane effect matrices, respectively, and δ_{ij} is the Kronecker delta function.

The characteristic quantities ρ, f, and c are chosen to non-dimensionalize the above equations. Then the governing parameters are obtained as follows: the heaving amplitude $A = A_0/c$, the frequency Reynolds number $Re_f = \rho f c^2/\mu$, the aspect ratio $H = R/c$, the stretching stiffness $S = Eh/(\rho f^2 c^3)$, the bending stiffness $K = EI/(\rho f^2 c^5)$, and the mass ratio of the plate and the fluid $M = \rho_s h/(\rho c)$.

The governing equations of the fluid–plate problem are solved numerically. When the immersed boundary (IB) method is applied to analyze flow–structure interaction, the body force term $\boldsymbol{f}$ in Eq. (2) is used as an interaction force between the boundary and the fluid to enforce the no-slip velocity boundary condition on the surface. The lattice Boltzmann equation with the body force model and non-uniform mesh technique are employed to solve the viscous fluid flow. Equation (4) for the deformable plate is solved by a finite element method and the deformation with large-displacement of the plate is handled by the corotational scheme [19].

After our careful convergence studies, the computational domain for fluid flow is chosen as $[-5, 15]\times[-6, 6]\times[-6, 6]$ in the x, y, and z directions. The finest lattice spacing is 0.025 in the near plate region and the coarsest spacing is 0.1 in the far boundary region. The plate is discretized by approximate 8000 triangular elements. The time step is $\Delta t = 0.0005$.

Based on a series of simulations, we have identified some typical movement states of the plate due to the fluid–plate interaction. The plate motion along the negative x-direction is mainly analyzed since the motion is related to the flapping-based locomotion of swimming and flying animals. In this study, some typical results are discussed for the parameters $A = 0.5$, $Re_f = 100$, $H = 2$, $K = 5$–1000, $S = 1000$ and $M = 2$. The dynamical behavior and propulsive performance are analyzed in terms of the mean propulsive speed, the propulsive efficiency, the passive pitching angle, and the Strouhal number.

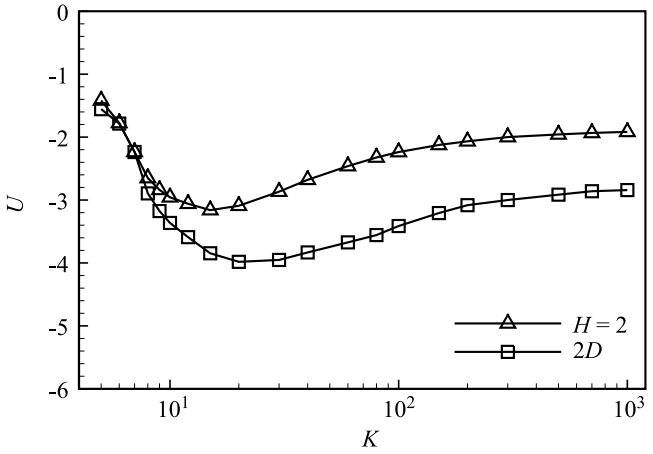

Fig. 2. The mean propulsive speed U versus the bending stiffness K.

We first analyze the behavior of the propulsive speed of the plate. Figure 2 shows the mean propulsive speed U versus the bending rigidity K for the 2D and 3D plates, where U is obtained by time average during steady locomotion. It is seen that the profiles of U are all concave up. The speed U decreases as K increases first, then reaches a minimum (corresponding to the maximum of $|U|$), and finally approaches a constant as K increases further. The forward speed $|U|$ for the 2D plate is overall larger than that for the 3D plate. Note that the motion of the flexible plate tends to the motion of the rigid one at large value of K, e.g. $K = 1000$. The forward speeds of the flexible plate are substantially greater than those of the corresponding rigid plate, indicating that the flexibility can improve the performance of forward propulsion.

The propulsive efficiency is investigated for the plate motion. As the plate spontaneously propels itself in the horizontal direction, the mean thrust becomes zero. To characterize the propulsive efficiency of a body in free motion, the ratio of the kinetic energy of the body motion and the work done by the deforming body over one flapping cycle T has been employed [9,13]. Then, the propulsive efficiency for the locomotion of flexible plate is expressed as

$$\eta = \frac{\frac{1}{2}MU^2}{\int_{t_0}^{t_0+T}\int_0^R\int_0^c \boldsymbol{F}_r(s_1, s_2, t)\cdot\frac{\partial \boldsymbol{X}(s_1,s_2,t)}{\partial t}\mathrm{d}s_1\mathrm{d}s_2\mathrm{d}t}, \tag{5}$$

where $\boldsymbol{F}_r(s_1, s_2, t)$ represents the force on the surrounding fluid by the plate and can be expressed as $\boldsymbol{F}_r(s_1, s_2, t) = -\boldsymbol{F}_s(s_1, s_2, t)$. As shown in Fig. 3 for the propulsive efficiency η, the efficiency first increases to a maximum and then decreases gradually as K increases for both the 2D and 3D plates. It is also identified that the efficiency η for the 2D plate is larger than that for the 3D plate. Similarly, there exists an optimal plate flexibility region for the maximal propulsive efficiency.

The passive pitching angle is associated with the deformation of the flexible plate and with hydrodynamic performance [3,20]. Figure 4 shows the root-mean-square (rms) value of the passive pitching angle α_{rms} for the 2D and 3D plates. The passive pitching angle is caused by the delayed motion of the free end of the plate relative to the constrained end. It is seen from Fig. 4 that smaller bending stiffness or more flexibility causes larger pitching angle. Comparing the profiles of α_{rms}, the pitching angles of the 3D plate are somewhat larger than those of the 2D plate for $K < 100$, and the pitching angles of the 2D and 3D plates tend to be together for $K > 100$.

Download English Version:

https://daneshyari.com/en/article/808222

Download Persian Version:

https://daneshyari.com/article/808222

Daneshyari.com